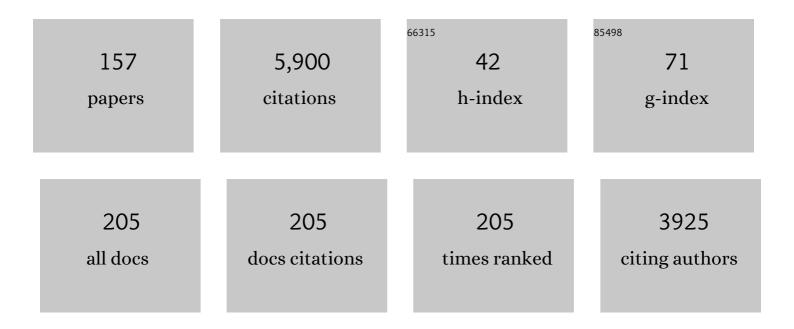
Matteo Massironi

List of Publications by Year in descending order

Source: https://exaly.com/author-pdf/6107939/publications.pdf Version: 2024-02-01



#	Article	IF	CITATIONS
1	The assessment of local geological factors for the construction of a Geogenic Radon Potential map using regression kriging. A case study from the Euganean Hills volcanic district (Italy). Science of the Total Environment, 2022, 808, 152064.	3.9	16
2	Spectral Units Analysis of Quadrangle H05â€Hokusai on Mercury. Journal of Geophysical Research E: Planets, 2022, 127, .	1.5	7
3	Geology of the Kuiper quadrangle (H06), Mercury. Journal of Maps, 2022, 18, 246-257.	1.0	7
4	Fundamental Science and Engineering Questions in Planetary Cave Exploration. Journal of Geophysical Research E: Planets, 2022, 127, .	1.5	8
5	Inception and Evolution of La Corona Lava Tube System (Lanzarote, Canary Islands, Spain). Journal of Geophysical Research: Solid Earth, 2022, 127, .	1.4	2
6	Equatorial grooves distribution on Ganymede: Length and self-similar clustering analysis. Planetary and Space Science, 2021, 195, 105140.	0.9	8
7	Long-term measurements of the erosion and accretion of dust deposits on comet 67P/Churyumov–Gerasimenko with the OSIRIS instrument. Monthly Notices of the Royal Astronomical Society, 2021, 504, 2895-2910.	1.6	7
8	Caldera Collapse as the Trigger of Chaos and Fractured Craters on the Moon and Mars. Geophysical Research Letters, 2021, 48, e2021GL092436.	1.5	8
9	Geologic Mapping and Age Determinations of Tsiolkovskiy Crater. Remote Sensing, 2021, 13, 3619.	1.8	3
10	Rheological and Mechanical Layering of the Crust Underneath Thumbprint Terrains in Arcadia Planitia, Mars. Journal of Geophysical Research E: Planets, 2021, 126, .	1.5	4
11	Dating long thrust systems on Mercury: New clues on the thermal evolution of the planet. Geoscience Frontiers, 2020, 11, 855-870.	4.3	13
12	Martian Ice Revealed by Modeling of Simple Terraced Crater Formation. Journal of Geophysical Research E: Planets, 2020, 125, e2019JE006108.	1.5	1
13	Lava tubes on Earth, Moon and Mars: A review on their size and morphology revealed by comparative planetology. Earth-Science Reviews, 2020, 209, 103288.	4.0	80
14	3D Extension at Plate Boundaries Accommodated by Interacting Fault Systems. Scientific Reports, 2020, 10, 8669.	1.6	3
15	Geological evolution of the Sinus Iridum basin. Planetary and Space Science, 2020, 194, 105134.	0.9	1
16	Time evolution of dust deposits in the Hapi region of comet 67P/Churyumov-Gerasimenko. Astronomy and Astrophysics, 2020, 636, A91.	2.1	13
17	An Integrated Geologic Map of the Rembrandt Basin, on Mercury, as a Starting Point for Stratigraphic Analysis. Remote Sensing, 2020, 12, 3213.	1.8	14
18	Mapping and Monitoring Urban Environment through Sentinel-1 SAR Data: A Case Study in the Veneto Region (Italy). ISPRS International Journal of Geo-Information, 2020, 9, 375.	1.4	17

#	Article	IF	CITATIONS
19	SIMBIO-SYS: Scientific Cameras and Spectrometer for the BepiColombo Mission. Space Science Reviews, 2020, 216, 1.	3.7	47
20	Rationale for BepiColombo Studies of Mercury's Surface and Composition. Space Science Reviews, 2020, 216, 1.	3.7	46
21	Global-scale brittle plastic rheology at the cometesimals merging of comet 67P/Churyumov–Gerasimenko. Proceedings of the National Academy of Sciences of the United States of America, 2020, 117, 10181-10187.	3.3	5
22	Spectrophotometric variegation of the layering in comet 67P/Churyumov-Gerasimenko as seen by OSIRIS. Astronomy and Astrophysics, 2019, 630, A16.	2.1	2
23	Structural Analysis of the Victoria Quadrangle Fault Systems on Mercury: Timing, Geometries, Kinematics, and Relationship with the Highâ€Mg Region. Journal of Geophysical Research E: Planets, 2019, 124, 2543-2562.	1.5	16
24	Surface Expressions of Subsurface Sediment Mobilization Rooted into a Gas Hydrate-Rich Cryosphere on Mars. Scientific Reports, 2019, 9, 8603.	1.6	12
25	Multidisciplinary analysis of the Hapi region located on Comet 67P/Churyumov–Gerasimenko. Monthly Notices of the Royal Astronomical Society, 2019, 485, 2139-2154.	1.6	9
26	Bilobate comet morphology and internal structure controlled by shear deformation. Nature Geoscience, 2019, 12, 157-162.	5.4	22
27	Rosetta/OSIRIS observations of the 67P nucleus during the April 2016 flyby: high-resolution spectrophotometry. Astronomy and Astrophysics, 2019, 630, A9.	2.1	6
28	Quantitative analysis of isolated boulder fields on comet 67P/Churyumov-Gerasimenko. Astronomy and Astrophysics, 2019, 630, A15.	2.1	4
29	The Rockyâ€Like Behavior of Cometary Landslides on 67P/Churyumovâ€Gerasimenko. Geophysical Research Letters, 2019, 46, 14336-14346.	1.5	9
30	Fluids mobilization in Arabia Terra, Mars: Depth of pressurized reservoir from mounds self-similar clustering. Icarus, 2019, 321, 938-959.	1.1	22
31	The geodynamic evolution of the Italian South Alpine basement from the Ediacaran to the Carboniferous: Was the South Alpine terrane part of the peri-Gondwana arc-forming terranes?. Gondwana Research, 2019, 65, 17-30.	3.0	19
32	Meter-scale thermal contraction crack polygons on the nucleus of comet 67P/Churyumov-Gerasimenko. Icarus, 2018, 301, 173-188.	1.1	33
33	Pre-Alpine and Alpine deformation at San Pellegrino pass (Dolomites, Italy). Journal of Maps, 2018, 14, 671-679.	1.0	3
34	Slip-tendency analysis as a tool to constrain the mechanical properties of anisotropic rocks. Journal of Structural Geology, 2018, 117, 136-147.	1.0	3
35	Mercury Hollows as Remnants of Original Bedrock Materials and Devolatilization Processes: A Spectral Clustering and Geomorphological Analysis. Journal of Geophysical Research E: Planets, 2018, 123, 2365-2379.	1.5	23
36	The big lobe of 67P/Churyumov–Gerasimenko comet: morphological and spectrophotometric evidences of layering as from OSIRIS data. Monthly Notices of the Royal Astronomical Society, 2018, 479, 1555-1568.	1.6	7

#	Article	IF	CITATIONS
37	Estimate of depths of source fluids related to mound fields on Mars. Planetary and Space Science, 2018, 164, 164-173.	0.9	13
38	Small Bodies and Dwarf Planets. , 2018, , 311-343.		0
39	Late movement of basin-edge lobate scarps on Mercury. Icarus, 2017, 288, 226-234.	1.1	16
40	Is the Linné impact crater morphology influenced by the rheological layering on the Moon's surface? Insights from numerical modeling. Meteoritics and Planetary Science, 2017, 52, 1388-1411.	0.7	5
41	Onset of N-Atlantic rifting in the Hoop Fault Complex (SW Barents Sea): An orthorhombic dominated faulting?. Tectonophysics, 2017, 706-707, 59-70.	0.9	14
42	The pristine interior of comet 67P revealed by the combined Aswan outburst and cliff collapse. Nature Astronomy, 2017, 1, .	4.2	100
43	The Colour and Stereo Surface Imaging System (CaSSIS) for the ExoMars Trace Gas Orbiter. Space Science Reviews, 2017, 212, 1897-1944.	3.7	111
44	Seasonal erosion and restoration of the dust cover on comet 67P/Churyumov-Gerasimenko as observed by OSIRIS onboard Rosetta. Astronomy and Astrophysics, 2017, 604, A114.	2.1	43
45	Modelling of the outburst on 2015 July 29 observed with OSIRIS cameras in the Southern hemisphere of comet 67P/Churyumov–Gerasimenko. Monthly Notices of the Royal Astronomical Society, 2017, 469, S178-S185.	1.6	12
46	Brittle ice shell thickness of Enceladus from fracture distribution analysis. Icarus, 2017, 297, 252-264.	1.1	19
47	The scattering phase function of comet 67P/Churyumov–Gerasimenko coma as seen from the Rosetta/OSIRIS instrument. Monthly Notices of the Royal Astronomical Society, 2017, 469, S404-S415.	1.6	44
48	The highly active Anhur–Bes regions in the 67P/Churyumov–Gerasimenko comet: results from OSIRIS/ROSETTA observations. Monthly Notices of the Royal Astronomical Society, 2017, 469, S93-S107.	1.6	30
49	Geomorphological and spectrophotometric analysis of Seth's circular niches on comet 67P/Churyumov–Gerasimenko using OSIRIS images. Monthly Notices of the Royal Astronomical Society, 2017, 469, S238-S251.	1.6	8
50	An extensional syn-sedimentary structure in the Early Jurassic Trento Platform (Southern Alps, Italy) as analogue of potential hydrocarbon reservoirs developing in rifting-affected carbonate platforms. Marine and Petroleum Geology, 2017, 79, 360-371.	1.5	6
51	Assessment of lithogenic radioactivity in the Euganean Hills magmatic district (NE Italy). Journal of Environmental Radioactivity, 2017, 166, 259-269.	0.9	16
52	The pebbles/boulders size distributions on Sais: Rosetta's final landing site on comet 67P/Churyumov–Gerasimenko. Monthly Notices of the Royal Astronomical Society, 2017, 469, S636-S645.	1.6	40
53	A three-dimensional modelling of the layered structure of comet 67P/Churyumov-Gerasimenko. Monthly Notices of the Royal Astronomical Society, 2017, 469, S741-S754.	1.6	22
54	Post-perihelion photometry of dust grains in the coma of 67P Churyumov–Gerasimenko. Monthly Notices of the Royal Astronomical Society, 2017, 469, S195-S203.	1.6	17

#	Article	IF	CITATIONS
55	Geologic mapping of the Comet 67P/Churyumov–Gerasimenko's Northern hemisphere. Monthly Notices of the Royal Astronomical Society, 2016, 462, S352-S367.	1.6	27
56	The southern hemisphere of 67P/Churyumov-Gerasimenko: Analysis of the preperihelion size-frequency distribution of boulders ≥7 m. Astronomy and Astrophysics, 2016, 592, L2.	2.1	27
57	Characterization of the Abydos region through OSIRIS high-resolution images in support of CIVA measurements. Astronomy and Astrophysics, 2016, 585, L1.	2.1	26
58	Sublimation of icy aggregates in the coma of comet 67P/Churyumov–Gerasimenko detected with the OSIRIS cameras on board <i>Rosetta</i> . Monthly Notices of the Royal Astronomical Society, 2016, 462, S57-S66.	1.6	23
59	Summer fireworks on comet 67P. Monthly Notices of the Royal Astronomical Society, 2016, 462, S184-S194.	1.6	112
60	Are fractured cliffs the source of cometary dust jets? Insights from OSIRIS/Rosetta at 67P/Churyumov-Gerasimenko. Astronomy and Astrophysics, 2016, 587, A14.	2.1	102
61	Regional surface morphology of comet 67P/Churyumov-Gerasimenko from Rosetta/OSIRIS images: The southern hemisphere. Astronomy and Astrophysics, 2016, 593, A110.	2.1	86
62	Detection of exposed H ₂ O ice on the nucleus of comet 67P/Churyumov-Gerasimenko. Astronomy and Astrophysics, 2016, 595, A102.	2.1	67
63	Aswan site on comet 67P/Churyumov-Gerasimenko: Morphology, boulder evolution, and spectrophotometry. Astronomy and Astrophysics, 2016, 592, A69.	2.1	53
64	Rosetta's comet 67P/Churyumov-Gerasimenko sheds its dusty mantle to reveal its icy nature. Science, 2016, 354, 1566-1570.	6.0	97
65	The Agilkia boulders/pebbles size–frequency distributions: OSIRIS and ROLIS joint observations of 67P surface. Monthly Notices of the Royal Astronomical Society, 2016, 462, S242-S252.	1.6	15
66	Geomorphological mapping of comet 67P/Churyumov–Gerasimenko's Southern hemisphere. Monthly Notices of the Royal Astronomical Society, 2016, 462, S573-S592.	1.6	23
67	The primordial nucleus of comet 67P/Churyumov-Gerasimenko. Astronomy and Astrophysics, 2016, 592, A63.	2.1	159
68	Geo-structural map of the Laguna Blanca basin (Southern Central Andes, Catamarca, Argentina). Journal of Maps, 2016, 12, 431-442.	1.0	2
69	Scientific assessment of the quality of OSIRIS images. Astronomy and Astrophysics, 2015, 583, A46.	2.1	67
70	Gravitational slopes, geomorphology, and material strengths of the nucleus of comet 67P/Churyumov-Gerasimenko from OSIRIS observations. Astronomy and Astrophysics, 2015, 583, A32.	2.1	113
71	Redistribution of particles across the nucleus of comet 67P/Churyumov-Gerasimenko. Astronomy and Astrophysics, 2015, 583, A17.	2.1	149
72	Regional surface morphology of comet 67P/Churyumov-Gerasimenko from Rosetta/OSIRIS images. Astronomy and Astrophysics, 2015, 583, A26.	2.1	153

#	Article	IF	CITATIONS
73	Geomorphology of the Imhotep region on comet 67P/Churyumov-Gerasimenko from OSIRIS observations. Astronomy and Astrophysics, 2015, 583, A35.	2.1	59
74	Size-frequency distribution of boulders ≥7 m on comet 67P/Churyumov-Gerasimenko. Astronomy and Astrophysics, 2015, 583, A37.	2.1	108
75	Geomorphology and spectrophotometry of Philae's landing site on comet 67P/Churyumov-Gerasimenko. Astronomy and Astrophysics, 2015, 583, A41.	2.1	41
76	Comet 67P/Churyumov-Gerasimenko: Constraints on its origin from OSIRIS observations. Astronomy and Astrophysics, 2015, 583, A44.	2.1	53
77	Temporal morphological changes in the Imhotep region of comet 67P/Churyumov-Gerasimenko. Astronomy and Astrophysics, 2015, 583, A36.	2.1	60
78	Integration of 3D modeling, aerial LiDAR and photogrammetry to study a synsedimentary structure in the Early Jurassic Calcari Grigi (Southern Alps, Italy). European Journal of Remote Sensing, 2015, 48, 527-539.	1.7	17
79	Fractures on comet 67P/Churyumovâ€Gerasimenko observed by Rosetta/OSIRIS. Geophysical Research Letters, 2015, 42, 5170-5178.	1.5	71
80	Lateral ramps and strike-slip kinematics on Mercury. Geological Society Special Publication, 2015, 401, 269-290.	0.8	11
81	Strike-Slip Faults. , 2015, , 2069-2078.		0
82	On the nucleus structure and activity of comet 67P/Churyumov-Gerasimenko. Science, 2015, 347, aaa1044.	6.0	366
83	The morphological diversity of comet 67P/Churyumov-Gerasimenko. Science, 2015, 347, aaa0440.	6.0	259
84	Geology of the Brenner Pass-Fortezza transect, Italian Eastern Alps. Journal of Maps, 2015, 11, 201-215.	1.0	7
85	Volcanism and tectonism across the inner solar system: an overview. Geological Society Special Publication, 2015, 401, 1-56.	0.8	46
86	Large heterogeneities in comet 67P as revealed by active pits from sinkhole collapse. Nature, 2015, 523, 63-66.	13.7	158
87	Phobos grooves and impact craters: A stereographic analysis. Icarus, 2015, 256, 90-100.	1.1	26
88	Are terrestrial plumes from motionless plates analogues to Martian plumes feeding the giant shield volcanoes?. Geological Society Special Publication, 2015, 401, 107-126.	0.8	11
89	Self-similar clustering distribution of structural features on Ascraeus Mons (Mars): implications for magma chamber depth. Geological Society Special Publication, 2015, 401, 203-218.	0.8	16
90	A cone on Mercury: Analysis of a residual central peak encircled by an explosive volcanic vent. Planetary and Space Science, 2015, 108, 108-116.	0.9	8

#	Article	IF	CITATIONS
91	Age dating of an extensive thrust system on Mercury: implications for the planet's thermal evolution. Geological Society Special Publication, 2015, 401, 291-311.	0.8	9
92	Two independent and primitive envelopes of the bilobate nucleus of comet 67P. Nature, 2015, 526, 402-405.	13.7	141
93	Age relationships of the Rembrandt basin and Enterprise Rupes, Mercury. Geological Society Special Publication, 2015, 401, 159-172.	0.8	14
94	High-Relief Ridge. , 2015, , 932-934.		2
95	Lobate Scarp. , 2015, , 1255-1262.		3
96	Search for satellites near comet 67P/Churyumov-Gerasimenko using Rosetta/OSIRIS images. Astronomy and Astrophysics, 2015, 583, A19.	2.1	13
97	High-Relief Ridge. , 2014, , 1-5.		Ο
98	In-situ high-temperature emissivity spectra and thermal expansion of C2/c pyroxenes: Implications for the surface of Mercury. American Mineralogist, 2014, 99, 786-792.	0.9	16
99	Spatial analysis of thickness variability applied to an Early Jurassic carbonate platform in the central Southern Alps (Italy): a tool to unravel synâ€sedimentary faulting. Terra Nova, 2014, 26, 239-246.	0.9	10
100	How multiple foliations may control large gravitational phenomena: A case study from the Cismon Valley, Eastern Alps, Italy. Geomorphology, 2014, 207, 149-160.	1.1	6
101	Strike-Slip Faults. , 2014, , 1-12.		0
102	Lobate Scarp. , 2014, , 1-11.		0
103	Olivine thermal emissivity under extreme temperature ranges: Implication for Mercury surface. Earth and Planetary Science Letters, 2013, 371-372, 252-257.	1.8	20
104	Geological map of the Middle Triassic Latemar platform (Western Dolomites, Northern Italy). Journal of Maps, 2013, 9, 313-324.	1.0	8
105	Geomorphology of the El Alamein Battlefield (Southern Front, Egypt). Journal of Maps, 2013, 9, 532-541.	1.0	4
106	On the nucleation of non-Andersonian faults along phyllosilicate-rich mylonite belts. Geological Society Special Publication, 2012, 367, 185-199.	0.8	23
107	Spectral analysis and geological mapping of the Daedalia Planum lava field (Mars) using OMEGA data. Icarus, 2012, 220, 679-693.	1.1	9
108	Mercury's radius change estimates revisited using MESSENGER data. Icarus, 2012, 221, 456-460.	1.1	39

#	Article	IF	CITATIONS
109	Dating deformation in the Gran Paradiso Massif (NW Italian Alps): Implications for the exhumation of high-pressure rocks in a collisional belt. Lithos, 2012, 144-145, 130-144.	0.6	26
110	(21) Lutetia spectrophotometry from Rosetta-OSIRIS images and comparison to ground-based observations. Planetary and Space Science, 2012, 66, 43-53.	0.9	31
111	The geomorphology of (21) Lutetia: Results from the OSIRIS imaging system onboard ESA's Rosetta spacecraft. Planetary and Space Science, 2012, 66, 96-124.	0.9	58
112	The cratering history of asteroid (21) Lutetia. Planetary and Space Science, 2012, 66, 87-95.	0.9	43
113	Geological map and stratigraphy of asteroid 21 Lutetia. Planetary and Space Science, 2012, 66, 125-136.	0.9	42
114	Physical properties of craters on asteroid (21) Lutetia. Planetary and Space Science, 2012, 66, 79-86.	0.9	41
115	Hydrocode simulations of the largest crater on asteroid Lutetia. Planetary and Space Science, 2012, 66, 147-154.	0.9	14
116	Images of Asteroid 21 Lutetia: A Remnant Planetesimal from the Early Solar System. Science, 2011, 334, 487-490.	6.0	179
117	Misoriented faults in exhumed metamorphic complexes: Rule or exception?. Earth and Planetary Science Letters, 2011, 307, 233-239.	1.8	31
118	Omeonga—A possible large impact structure on the Eastern Kasai Province (D.R. Congo)?. Meteoritics and Planetary Science, 2011, 46, 1804-1813.	0.7	2
119	A New Stereo Algorithm based on Snakes. Photogrammetric Engineering and Remote Sensing, 2011, 77, 495-507.	0.3	4
120	The effects of the target material properties and layering on the crater chronology: The case of Raditladi and Rachmaninoff basins on Mercury. Planetary and Space Science, 2011, 59, 1968-1980.	0.9	51
121	Thermochronological evidence for a late Pliocene climate-induced erosion rate increase in the Alps. International Journal of Earth Sciences, 2011, 100, 847-859.	0.9	12
122	Influence of the antiformal setting on the kinematics of a large mass movement: the Passo Vallaccia, eastern Italian Alps. Bulletin of Engineering Geology and the Environment, 2011, 70, 497-506.	1.6	9
123	The Latemar: A Middle Triassic polygonal fault-block platform controlled by synsedimentary tectonics. Sedimentary Geology, 2011, 234, 1-18.	1.0	41
124	Mapping the Buraburi granite in the Himalaya of Western Nepal: Remote sensing analysis in a collisional belt with vegetation cover and extreme variation of topography. Remote Sensing of Environment, 2011, 115, 1129-1144.	4.6	57
125	Observing Mercury: from Galileo to the stereo camera on the BepiColombo mission. Proceedings of the International Astronomical Union, 2010, 6, 213-218.	0.0	1
126	SIMBIO-SYS: The spectrometer and imagers integrated observatory system for the BepiColombo planetary orbiter. Planetary and Space Science, 2010, 58, 125-143.	0.9	70

#	Article	IF	CITATIONS
127	The cratering history of asteroid (2867) Steins. Planetary and Space Science, 2010, 58, 1116-1123.	0.9	46
128	Benefits of the Proposed Magia Mission for Lunar Geology. Earth, Moon and Planets, 2010, 107, 267-297.	0.3	0
129	Three-dimensional characterization of a crustal-scale fault zone: The Pusteria and Sprechenstein fault system (Eastern Alps). Journal of Structural Geology, 2010, 32, 2022-2041.	1.0	43
130	Mercury's surface and composition to be studied by BepiColombo. Planetary and Space Science, 2010, 58, 21-39.	0.9	31
131	Beagle Rupes – Evidence for a basal decollement of regional extent in Mercury's lithosphere. Icarus, 2010, 209, 256-261.	1.1	27
132	Evidence for Young Volcanism on Mercury from the Third MESSENGER Flyby. Science, 2010, 329, 668-671.	6.0	118
133	Correction to "Mercury's geochronology revised by applying Model Production Function to Mariner 10 data: Geological implications― Geophysical Research Letters, 2010, 37, n/a-n/a.	1.5	1
134	Laser scanning-based recognition of rotational movements on a deep seated gravitational instability: The Cinque Torri case (North-Eastern Italian Alps). Geomorphology, 2010, 122, 191-204.	1.1	113
135	A NEW CHRONOLOGY FOR THE MOON AND MERCURY. Astronomical Journal, 2009, 137, 4936-4948.	1.9	152
136	Inflated flows on Daedalia Planum (Mars)? Clues from a comparative analysis with the Payen volcanic complex (Argentina). Planetary and Space Science, 2009, 57, 556-570.	0.9	25
137	Use of PSInSARâ,,¢ data to infer active tectonics: Clues on the differential uplift across the Giudicarie belt (Central-Eastern Alps, Italy). Tectonophysics, 2009, 476, 297-303.	0.9	28
138	Mercury's geochronology revised by applying Model Production Function to Mariner 10 data: Geological implications. Geophysical Research Letters, 2009, 36, .	1.5	23
139	THE STEREO CAMERA ON THE BEPICOLOMBO ESA/JAXA MISSION: A NOVEL APPROACH. , 2009, , 305-322.		16
140	Simulations using terrestrial geological analogues to assess interpretability of potential geological features of the Hermean surface restituted by the STereo imaging Camera of the SIMBIOSYS package (BepiColombo mission). Planetary and Space Science, 2008, 56, 1079-1092.	0.9	10
141	3D fold and fault reconstruction with an uncertainty model: An example from an Alpine tunnel case study. Computers and Geosciences, 2008, 34, 351-372.	2.0	57
142	Interpretation and processing of ASTER data for geological mapping and granitoids detection in the Saghro massif (eastern Anti-Atlas, Morocco). , 2008, 4, 736.		66
143	Evolution of a poly-deformed relay zone between fault segments in the eastern Southern Alps, Italy. Geological Society Special Publication, 2007, 290, 351-366.	0.8	20
144	Miocene to present major fault linkages through the Adriatic indenter and the Austroalpine—Penninic collisional wedge (Alps of NE Italy). Geological Society Special Publication, 2006, 262, 245-258.	0.8	21

#	Article	IF	CITATIONS
145	Geodetic and hydrological aspects of the Merano earthquake of 17 July 2001. Journal of Geodynamics, 2005, 39, 317-336.	0.7	25
146	MEMORIS: a wide angle camera for the BepiColombo mission. Advances in Space Research, 2004, 33, 2182-2188.	1.2	3
147	Large-scale fault kinematic analysis in Noctis Labyrinthus (Mars). Planetary and Space Science, 2004, 52, 215-222.	0.9	19
148	Average strain rate in the Italian crust inferred from a permanent GPS network - II. Strain rate versus seismicity and structural geology. Geophysical Journal International, 2003, 155, 254-268.	1.0	43
149	Geological outline of the Alps. Episodes, 2003, 26, 175-180.	0.8	177
150	Polyphase Tertiary fault kinematics and Quaternary reactivation in the central-eastern Alps (western) Tj ETQq0 0 0	rgBT /Ov	erlgck 10 Tf
151	The Aosta–Ranzola extensional fault system and Oligocene–Present evolution of the Austroalpine–Penninic wedge in the northwestern Alps. International Journal of Earth Sciences, 2001, 90, 654-667.	0.9	56
152	Miocene to Present kinematics of the NW-Alps: evidences from remote sensing, structural analysis, seismotectonics and thermochronology. Journal of Geodynamics, 2000, 30, 205-228.	0.7	29
153	Post-nappe brittle tectonics and kinematic evolution of the north-western Alps: an integrated approach. Tectonophysics, 2000, 327, 267-292.	0.9	46
154	THE â€ [¬] MOON MAPPING' PROJECT TO PROMOTE COOPERATION BETWEEN STUDENTS OF ITALY AND CHINA. International Archives of the Photogrammetry, Remote Sensing and Spatial Information Sciences - ISPRS Archives, 0, XLI-B6, 71-78.	0.2	6
155	THE â€ [¬] MOON MAPPINGâ€ [™] PROJECT TO PROMOTE COOPERATION BETWEEN STUDENTS OF ITALY AND CHINA. International Archives of the Photogrammetry, Remote Sensing and Spatial Information Sciences - ISPRS Archives, 0, XLI-B6, 71-78.	0.2	4
156	A comet in Alpine style: how standard techniques for the reconstruction of geological structures, pioneered by Émile Argand, can help unravelling the evolution of the Solar System. Rendiconti Online Societa Geologica Italiana, 0, 37, 34-36.	0.3	0
157	A hidden Oligocene pluton linked to the Periadriatic Fault System beneath the Permian Bressanone pluton, eastern Southern Alps, International Geology Review, 0, , 1-20,	1.1	0